Am J Cancer Res 2024;14(1):114-129
www.ajcr.us /ISSN:2156-6976/ajcr0152111

Original Article

miR-99b/let-7e/miR-125a cluster suppresses pancreatic cancer through regulation of NR6A1

Yaoqing Li[1], Guolin Zhang[1], Chuchu Xu[1], Liyijing Shen[2], Guangen Xu[1], Kewei Ji[1], Zhiqiang Lin[3]

[1]Department of Gastrointestinal Surgery, Shaoxing People's Hospital, Shaoxing 312000, Zhejiang, P. R. China; [2]Department of Radiology, Shaoxing People's Hospital, Shaoxing 312000, Zhejiang, P. R. China; [3]Department of Vascular Hernia Surgery, Shaoxing People's Hospital, Shaoxing 312000, Zhejiang, P. R. China

Received July 9, 2023; Accepted December 8, 2023; Epub January 15, 2024; Published January 30, 2024

Abstract: This experiment investigates how the miR-99b/let-7e/miR-125a cluster regulates the mechanism of NR6A1 involved in the invasive and metastatic effects of pancreatic cancer (PCa). Bioinformatics prediction and dual luciferase reporter gene assay were applied to verify the targeted relationship between miR-99b/let-7e/miR-125a and NR6A1. ASPC1 cells underwent transfection with lentiviruses to overexpress miR-99b/let-7e/miR-125a (individual or together) to explore functions of miR-99b/let-7e/miR-125a cluster governing NR6A1 in PCa. The detection of tumorigenesis was verified by tumor formation assay in nude mice in vivo, and mouse models of liver metastasis of PCa observed cell metastasis of PCa. MiR-99b/let-7e/miR-125a cluster was screened for differential expression in PCa. NR6A1 was confirmed as a target gene of the miR-99b/let-7e/miR-125a cluster. Findings demonstrated that overexpression of the miR-99b/let-7e/miR-125a cluster inhibited cell invasion, metastasis, proliferation, and tumorigenesis in PCa. Conversely, overexpressed NR6A1, a crucial gene in the miR-99b/let-7e/miR-125a cluster, promoted cell invasion, migration, and proliferation in PCa. Moreover, the overexpression of the miR-99b/let-7e/miR-125a cluster inhibited liver metastases and tumor formation. Thus, the study concludes that the miR-99b/let-7e/miR-125a cluster impedes the invasion and metastasis of PCa cells via targeting the NR6A1 gene.

Keywords: miR-99b/let-7e/miR-125a, NR6A1, pancreatic cancer, invasion, migration, neural infiltration

Introduction

Pancreatic cancer (PCa), known for its high malignancy, poses formidable challenges in treatment and prognosis, primarily due to its propensity for aggressive invasion and metastasis [1]. Clinically, many patients with PCa, are often accompanied by elevated levels of alkaline phosphatase and circulating bilirubin [2-4]. Studies on the molecular pathogenesis of PCa suggest that genetic alterations (i.e., K-ras mutations), particularly epigenetic dysregulation of tumor-associated genes, are considered a hallmark of PCa [5]. In recent years, prostate cancer's molecular and genetic basis has become increasingly understood, but due to its aggressive nature, lack of early diagnostic and prognostic biomarkers, late clinical presentation, and limited efficacy of available therapies (i.e., chemotherapy and radiotherapy) [6-8]. PCa is usually advanced during detection, resulting in a poor prognosis and a high mortality rate [9]. Although more specific treatments (i.e., tumor-specific targeted therapies) have recently been applied, only patients with small tumor sizes and complete surgical resection have a better chance of survival [10]. Therefore, detecting new biomarkers and molecular targets is crucial for diagnosing and treating prostate cancer.

MicroRNAs (miRNAs) are a class of small, non-coding RNAs that have been implicated in the tumorigenesis and metastasis of various cancers [11]. Among them, microRNA-99b (miR-99b), a member of the miR-99 family, has been reported to suppress the expression of prostate-specific antigens and inhibit the proliferation of prostate cancer cells [12, 13]. Furthermore, miR-125a, belonging to the miR-10 family, has been shown to foster resistance to gemcitabine in PCa cells by targeting A20 [14]. miR-125a belongs to the miR-10 family, which includes two homologs (hsa-miR-125b-1,

hsa-miR-125b-2) that play key roles in various molecular and cellular processes, such as differentiation, proliferation, apoptosis, and regulation of matrix metalloproteinases [15]. let-7 was first identified in 2000 and is the second miRNA identified after lin-4, which has 13 family members with the same sequence homology in the seed region, most of which are associated with the regulation of cancer drug sensitivity [16]. Recently, ZEB1 was found to induce the expression of miR-99b/let-7e/125a involved in invasive metastasis of esophageal squamous carcinoma cells [17]. NR6A1 is an important orphan nuclear receptor associated with disease progression, aggressiveness prediction, and prostate cancer treatment [18]. However, the regulatory role of these miRs in the development and progression of cancers, including PCa, remains unknown.

To elucidate the role of the miR-99b/let-7e/miR-125a cluster in PCa, we investigated their expression profiles and targeted interaction with NR6A1 using diverse experimental methodologies. Additionally, we assessed their impact on the invasion and metastasis of PCa cells. Our results suggest that the miR-99b/let-7e/miR-125a cluster can inhibit PCa invasion and metastasis by regulating the expression of the NR6A1 gene. These results may provide important insights into developing novel PCa therapeutic agents and treating PCa.

Materials and methods

Bioinformatics

"Pancreatic cancer" was used as a keyword to retrieve the gene expression microarray dataset of PCa-related genes in the GEO database (http://www.ncbi.nlm.nih.gov/geo). The differentially expressed genes of the microarray dataset expression matrix were identified using the Limma package in R language [19]. The image was drawn with the screening conditions $P < 0.05$ and |LogFoldChange| > 2.0. Website miRdb (http://www.mirdb.org/) was used to predict the target genes of miRNA.

Research subjects

Cell lines: Normal pancreatic duct epithelial cell line (HPDE) and human PCa cell lines (SW1990, PANC-1, BxPC-3, and ASPC1) were used in this study. All these cell lines, obtained from the American Type Culture Collection (ATCC, Rockville, Maryland, USA) were cultured for under six months. The cells were cultured in RPMI1640 medium containing 10% fetal bovine serum (FBS) and 1% antibiotics/antifungal agents and then placed in an incubator at 37°C with 5% CO_2.

Clinical samples: 38 PCa tissue samples and 10 adjacent normal control tissue samples were collected from our hospital. Informed consent was obtained from each participant, and the study was approved by the ethics committee (Approval No. 2022-148-Y-02).

Luciferase report assay

A dual-luciferase assay validated the targeting relationship between miR-99b/let-7e/miR-125a and NR6A1 gene. PCa cells were seeded in a 24-well plate 24 hours before transfection. The cells were divided into three groups: the wild-type plasmid group, the mutant plasmid group, and the negative control group. The wild-type plasmid group was transfected with miR-99b, let-7e, miR-125a, miR-99b/let-7e/miR-125a mimic, and a mutant luciferase reporter plasmid derived from the NR6A1 3'UTR. The mutant plasmid group was transfected with miR-99b, let-7e, miR-125a, miR-99b/let-7e/miR-125a mimic, and mutant luciferase reporter plasmid NR6A1 3'WT. Cells were transfected for the negative control group, with miR-99b, let-7e, miR-125a, miR-99b/let-7e/miR-125a mimic, and a control luciferase plasmid. Twenty-four hours post-transfection, luciferase activity was measured using the dual-luciferase reporter assay. This experiment was independently replicated three times, with six replicates for each trial.

Transfection of miRNA mimics, inhibitors, siRNAs, and plasmid

The PCa cell line ASPC1 was cultured in DMEM (Hy Clone, Ogden, UT, USA), supplemented with 10% fetal bovine serum, in an incubator at 37°C with 5% CO_2 and saturated humidity. When 80% confluence was reached, the cells were detached using 0.25% trypsin for passaging. PCa cells in the logarithmic growth phase were adjusted to a cell density of 10^7 cells/L, seeded in 6-well plates, with 2 mL of cell suspension added to each well, and cells were transfected according to the instructions of

Table 1. Primer sequences of miR-99b, let-7e, miR-125a, NR6A1, U6 and *β*-actin in RT-qPCR

Gene	Primer sequences
miR-99b	F: 5'-ATCC AGTGCGTGTCGTG-3'
	R: 5'-TGCTCAAGCT CGTGTCTGT-3'
let-7e	F: 5'-TGAGGTAGGAGGTTGT-3'
	R: 5'-TATCCAGTGCGTGTCGTGGA-3'
miR-125a	F: 5'-ACACTCCAGCTGGGACAGGTGAGGTTCTTG-3'
	R: 5'-CTCAACTGGTGTCGTGGAGTCGGCAATTCAGTTGAGGGCTCCCA-3'
NR6A1	F: 5'-GGGATGAACCGGAAGGCTATC-3'
	R: 5'-GGCTGGTTGCTCTCCGAAG-3'
U6	F: 5'-AAAGCAAATCATCGGACGACC-3'
	R: 5'-GTACAACACATTGTTTCCTCGGA-3'
β-actin	F: 5'-CGTGACATTAAGGAGAAGCTG-3'
	R: 5'-CTAGAAGCATTTGCGTGGAC-3'

Note: RT-qPCR, reverse transcription quantitative polymerase chain reaction; miR-99b, microRNA-99b; miR-125a, microRNA-125a; F, forward; R, reverse.

lipofectamin2000 (11668019, Thermo Fisher Scientific, USA) when the cell density grew to 30-50%. PCa cells were transfected with 100 nM miRNA mimics (99b/7e/125a), miRNA mixture (33 nM of each miRNA) or negative control (NC); 120 nM miRNA inhibitor mixture (99b/7e/125a-i) or negative control (NC-i); 60 nM NR6A1 siRNA. Two siRNAs targeting NR6A1 were used in this study. The sequences of siRNA-1 were as follows: sense, 5'-GAGCAACCAUGGUGAUAGUTT-3'; and antisense, 5'-ACUAUCACCAUGGUUGCUCTT-3'. The sequences of siRNA-2: sense were, 5'-CCUCCACAUUACCAAUAUATT-3'; and antisense, 5'-UAUAUUGGUAAUGUGGAGGTT-3'. The siRNA NC (negative control) was used with the following sequences: sense, 5'-UUCUCCGAACGUGUCACGUTT-3'; and antisense, 5'-ACGUGACACGUUCGGAGAATT-3'. All miRNA mimics, inhibitors, and siRNAs were synthesized by RiboBio (Guangzhou, China) and transfected using HiPerFect transfection reagent (QIAGEN).

Virus infection

For miRNA screening, ASPC1 cells were plated in a 6-well plate at a density of 2×10^5 cells per well one day before infection. The Lenti-miRTM virus (SBI, Mountain View, CA, USA) was diluted at an MOI of 3 and added with polybrene to a final 5 μg/ml concentration in the cell medium. Next, ASPC1 cells were infected with lentivirus overexpressing miR-99b/let-7e/miR-125a (individual or cluster) or negative control (GeneChem, Shanghai, China) and selected with 1 μg/ml puromycin.

RT-qPCR

Total RNA was extracted using the miRNeasy Mini Kit (217004, QIAGEN, Hilden, Germany). The concentration and purity of the total RNA were determined using a Nanodrop 2000 micro ultraviolet spectrophotometer (1011U, Nanodrop, USA) based on the A260/A230 and A260/A280 ratios. The cDNA was synthesized by TaqMan MicroRNA Reverse Transcription Primer (4427975, Applied Biosystems, Carlsbad, CA, USA) according to the manufacturer's recommendation. In detail, the cDNA was diluted to a concentration of 50 ng/μL. For each reaction, 2 μL diluted cDNA was added into the reaction system, and the total volume was 25 μL. Reverse transcription was performed at 37°C for 30 min and 85°C for 5 s. miR-125a, miR-99b, let-7e, and NR6A1 were provided by TaKaRa Company (Otsu Shinga, Japan) (**Table 1**). RT-qPCR was conducted using an ABI7500 quantitative PCR instrument (7500, ABI, Carlsbad, CA, USA). In detail, predenaturization was performed at 95°C for 10 min, followed by denaturization for 40 cycles at 95°C for 10 s. Then, annealing was conducted at 60°C for 20 s, followed by extension for 40 cycles at 72°C for 34 s. The reaction system is composed of 0.8 μL PCR Reverse Primer (10 μM), 0.8 μL PCR Forward Primer (10 μM), 10 μL SYBR Premix Ex TaqTM II, 0.4 μL ROX Reference Dye, 2.0 μL cDNA templates, and 6.0 μL distilled water. U6 was taken as the internal reference of miR-99b, let-7e, and miR-125a, whereas β-actin was the internal reference of NR6A1. The $2^{-\Delta\Delta Ct}$ indicated the ratio of the expression of the target gene between the experimental group and the control group.

Western blot

PCa cells were collected, total cell protein was extracted, and a 2D Quant kit was used for protein quantification. Approximately 50 ug of pro-

tein samples were taken for SDS-PAGE, transferred to the membrane, closed, and incubated overnight at 4°C with rabbit anti-NR6A1 (ab38816, 1:250), MMP-2 (ab37150, 1:500), MMP-9 (ab38898, 1:1000), and VEGF (ab39256, 1:1000) (all the above antibodies were purchased from Abcam, USA). Subsequently, the membrane was incubated with IgG goat anti-rabbit secondary antibody (A21020, Abbkine, USA) (1:1000 dilution) at 37°C for 1 h. The membrane was then washed thrice with phosphate buffer saline (PBS) for 5 min before developing. Glyceraldehyde-phosphate dehydrogenase (GAPHD) was taken as the internal reference. The relative protein expression level was calculated as the ratio of the gray value of the target protein band to that of the internal reference band.

Transwell assay

In this experiment, 200 μL melted Matrigel gel (YB356234, Shanghai Yu Bo Biotech Co., Limited, Shanghai, China) was mixed with an equal volume of the serum-free medium at 4°C, transferred to the upper chamber of the transwell plate (50 μL/well) and placed in an incubator for 2-3 h for solidification. Cells were digested, counted, and suspended in 20% FBS. Cell suspension (200 μL) was added to the upper chamber of each well, while 800 μL 20% FBS was added to the lower chamber. The solution was then incubated at 37°C for 20-24 h. After incubation, the plates were washed with PBS twice and soaked for 10 min in formaldehyde, followed by washing with distilled water thrice. Then, cells were stained with 0.1% crystal violet, stilled for 30 min at room temperature, and washed with PBS twice. A cotton swab was used to remove cells external to the membrane. Finally, cells were observed, photographed, and counted under an inverted microscope. No basal Matrigel was needed for the Transwell assay, and the cells were only incubated for 16 h.

EdU incorporation assay

PCa cells in the logarithmic phase, ranging from 2×10^3-4×10^4 cells per well, were inoculated in 96-well plates and cultured to the expected growth stage. Twenty-four hours later, the attached cells were transfected as 3 wells per group. After 48 h, cells were labeled with EdU and incubated with a medium containing 100 μL EDU for 2 h. Labeled cells were then incubated with 100 μL cell fixation buffer for 30 min at room temperature after washing with PBS twice. Then, the fixed cells were mixed with 2 mg/mL glycine, incubated for 5 min, and washed with 100 μL PBS for 5 min. After washing, cells were cultured with penetration reagent (PBS containing 0.5% TritonX-100, 100 μL/well) and washed with PBS. The cells were mixed with 1 × Apollo staining solution and incubated for 30 min, avoiding exposure to light. Then, penetration reagent was added to the cells, followed by methanol washing. After penetration, cells were mixed with 1 × Hoechst 33342 reaction buffer (100 μL/well), decolorized, and incubated for 30 min at room temperature, avoiding exposure to light, followed by PBS (100 μL/well) washing thrice. Finally, cells were stained and mixed with an anti-fade mounting medium (100 μL/well). In this experiment, six to ten fields in each well were randomly selected, photographed, and observed under a fluorescence microscope.

Animal experiment

BALB/c nude mice (6 weeks old) were obtained from Zhaoyan (Suzhou) New Drug Research Center Ltd., China, and housed in a specific pathogen-free environment. The catalog number for the mice was i-003. Female nude mice without thymus were subcutaneously inoculated with stable overexpression of miR-99b/let-7e/miR-125a cluster or negative control PCa cell line. The nude mice were maintained in an environment with a constant temperature (25-27°C) and humidity (45%-50%). After transfection, cells were digested and centrifuged when the confluence reached 80%-90%. After washing with PBS 2 to 3 times, adjust the concentration of cell suspension to 1×10^7 cells/mL. Then, 20 μl cell suspension was inoculated subcutaneously in nude mice (5 mice/group). Finally, the mice were sacrificed using CO_2 after 6 weeks, and the size and weight of the transplanted tumor were measured.

Nude mice were injected through the caudal vein by 4', 6-diamidino-2-phenylindole (DAPI) labeled PCa cell lines (i.e., miR-99b/let-7e/miR-125a cluster) or NC as to establish a PCa model (5 mice/group). The concentration of PCa cells in the logarithmic growth phase was then adjusted to 2×10^7 cells/mL and incubated with the fluorescent dye DAPI (10 μg/L) (37°C

for 5 min and 4°C for 15 min). After washing with PBS, cells were centrifuged at 402 × g for 5 min and resuspended in physiological saline solution (2 × 10^7 cells/mL). Nude mice were injected with 0.1 mL labeled cells through the caudal vein and sacrificed by CO_2 after 8 weeks. The livers were harvested to evaluate the tumor metastasis, and the IVIS Lumina II system (Caliper LifeSciences, Waltham, MA, USA) was used to observe the fluorescence. All animal experiments met the requirements of the ethics committee (2022-148--Y-01).

Statistics

These analyses were performed with the SPSS Version 17.0 statistical software package. Differences between the two groups were compared using Pearson. The Spearman coefficients test analyzed the correlation between miRNA level and clinical stages. The Spearman coefficients test analyzed the correlation between miRNA level and clinical stages.

Results

miR-99b/let-7e/miR-125a is a cluster of differentially expressed miRNAs in PCa

The data analysis results of the GSE50632 and GSE41369 chips revealed that miR-125a, let-7e, and miR-99b exhibited low expression in PCa (**Figure 1A**). miR-125a, let-7e and miR-99b were derived from miRNA clusters located within a ~750 base pair region on human chromosome 19 (**Figure 1B**). We examined the expression of miR-125a, let-7e, and miR-99b in PCa, pancreatitis (CP), and regular pancreatic patients. RT-qPCR results showed that the expression of miR-125a, let-7e, and miR-99b was significantly lower in PCa than in the CP and Normal groups (**Figure 1C-E**). We examined and analyzed the correlation between the varying expression levels of miR-125a, let-7e, and miR-99b in PCa and various clinicopathological factors, and the results showed that the expression levels of let-7e and miR-99b were associated with Perineural invasion, Lymph node metastasis and TNM stage of PCa. In contrast, the expression level of miR-125a correlated with tumor size and perineural invasion of PCa (**Table 2**). We also examined the mRNA expression of miR-125a, let-7e, and miR-99b in normal pancreatic ductal epithelial cells (HPDE) and human PCa cell lines (PanC-1, Mia Paca-2, and HEK-293T), and the results showed that miR-125a, let-7e, and miR-99b were significantly lower than those in normal pancreatic ductal epithelial cells (HPDE). 7e and miR-99b expression were decreased in PCa cell lines SW1990, PANC-1, BxPC-3, and ASPC1 in order, with ASPC1 PCa expression being the lowest, which was selected for the following cellular experiments.

The miR-99b/let-7e/miR-125a cluster inhibits malignant features of PCa cells

To determine the potential role of miR-99b/let-7e/miR-125a in PCa cells, we first overexpressed them by transfecting PCa cells with miRNA mimics. The results showed that the expression of miR-99b, let-7e, and miR-125 was increased in the miR-99b/let-7e/miR-125 group compared to the NC group. Additionally, transfecting miR-99b, let-7e, or miR-125 mimics significantly enhanced the corresponding miRNA expression (**Figure 2A**). We performed Transwell assays to assess PCa cells' invasiveness and migration ability and EdU staining to evaluate their proliferative capacity. As depicted in **Figure 2B**, **2C**, overexpressing the three miRNAs individually or together suppressed cell invasion, migration, and proliferation. Similarly, through lentivirus infection, stable expression of miR-99b/let-7e/miR-125a was achieved in ASPC1 cells. The results showed increased expression of miR-99b, let-7e, and miR-125 in the Cluster group compared to the NC group. Furthermore, the miR-99b/let-7e/miR-125-i group exhibited decreased expression of miR-99b, let-7e, and miR-125 compared to the NC-i group (**Figure 2D**, **2E**), PCa cells exhibited a solid ability for invasion, migration, and proliferation (**Figure 2F-H**). We also examined the expression of metastasis-related proteins using Western blot. The results showed that the miR-99b/let-7e/miR-125a cluster showed significantly lower MMP-2, MMP-9, and VEGF expression than the corresponding NC group. In comparison, the addition of miR-99b/let-7e/miR-125 inhibitor resulted in significantly lower expression of MMP-2, MMP-9 and VEGF expression was significantly increased after the addition of miR-99b/let-7e/miR-125 inhibitor (**Figure 2I**). These results suggest that miR-99b/let-7e/miR-125a inhibits cells' invasive and metastatic ability in vitro.

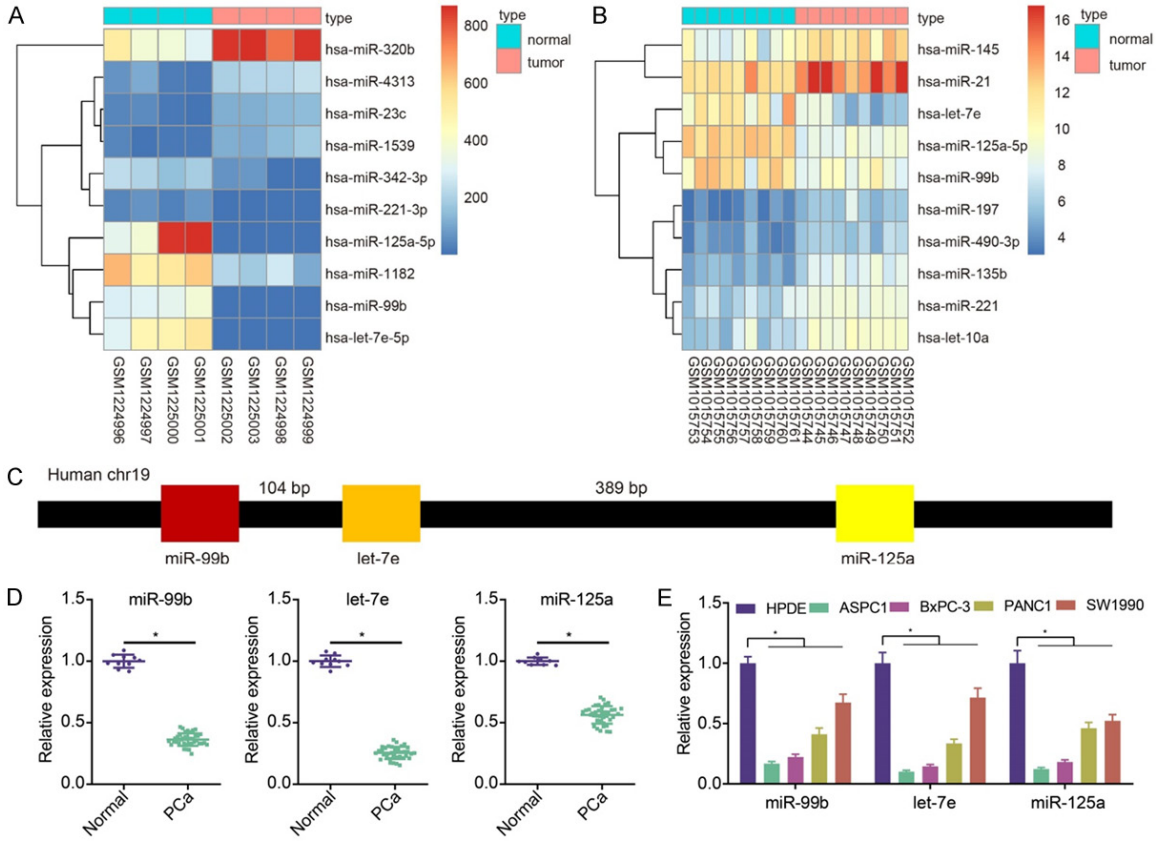

Figure 1. miR-99b/let-7e/miR-125a cluster is downregulated in PCa. A. The image of microarray dataset GSE50632. B. The image of microarray dataset GSE41369. The horizontal axis represents the number of samples, whereas the vertical axis represents the name of the differential gene. The upper right column is the color gradation with color reflecting gene-chip expression values. In the column, each rectangle corresponds to a sample value, whereas each row represents the expression of all genes in a sample. The dendrogram on the left side is an analysis of gene expression of different samples. In the graph, the bar on the top marks the sample type and the upper right box demonstrates the reference of sample color. In particular, sample with the blue color was taken as the normal control, whereas the red was as the sample with tumor. C. Illustration of miR-99b/let-7e/miR-125a cluster on human chromosome. D. RT-qPCR analysis of the expressions of miR-125a, let-7e and miR-99b in patients with PCa and normal pancreas; N (normal group) = 10; N (PCa group) = 38; A paired t-test was employed to compare the data from cancer tissue and adjacent noncancerous tissue, with $P < 0.05$ indicating statistical significance. E. RT-qPCR analysis of the expressions of miR-125a, let-7e and miR-99b in normal human HPDE cells and human PCa cell lines (SW1990, PANC-1, BxPC-3 and ASPC1); A one-way analysis of variance (ANOVA) was conducted to compare the data among multiple groups, with $P < 0.05$ indicating statistical significance when compared to normal pancreatic ductal epithelial cells (HPDE). The experiment was repeated three times.

NR6A1 is the target gene of the miR-99b/let-7e/miR-125a cluster

To investigate the potential target genes of miR-99b/let-7e/miR-125a cluster, we predicted the target genes of miR-125a, let-7e, and miR-99b by miRdb website (http://www.miRdb.org/), and found that NR6A1 was the target gene of miR-125a, let-7e and miR-99b (**Figure 3A**). We also used RNA22 (https://cm.jefferson.edu/RNA22) online predictive analysis database, and the predictive analysis verified the presence of binding sites of miR-99b, let-7e, miR-125a and NR6A1 3'UTR (**Figure 3B**), therefore, we focused on NR6A1 for further study. To confirm that NR6A1 is a direct target gene of miR-99b/let-7e/miR-125a, target validation was performed using a dual luciferase reporter, and the experimental results showed that the luciferase activity of NR6A1 wild-type 3'-UTR was significantly inhibited by miR-125a, let-7e, miR-99b and miR-99b/let-7e/miR-125a mimics compared with the NC group ($P < 0.05$), whereas the luciferase activity of mutant 3'-UTR was not inhibited (**Figure 3C**). In addition, NR6A1 mRNA and protein levels were

Table 2. Relationship between the expression of miR-99b, let-7e, miR-125a and clinical features

Variable	n	miR-99b		*P*-value	let-7e		*P*-value	miR-125a		*P*-value
		Low	High		Low	High		Low	High	
Age				0.737			0.737			0.74
< 60	14	8	6		6	8		7	7	
≥ 60	24	11	13		13	11		10	14	
Gender				0.515			0.515			0.752
Male	21	9	12		9	12		10	11	
Female	17	10	7		10	7		7	10	
Tumor size				0.515			1.000			0.048
< 3 cm	21	9	12		10	11		6	15	
≥ 3 cm	17	10	7		9	8		11	6	
Perineural invasion				0.038			0.038			0.015
Negative	13	3	10		3	10		2	11	
Positive	25	16	9		16	9		15	10	
Lymph node metastasis				0.029			0.003			1.000
Negative	11	2	9		1	10		5	6	
Positive	27	17	10		18	9		12	15	
TNM stage				0.045			< 0.001			0.744
I-II	15	4	11		2	13		6	9	
III-IV	23	15	8		17	6		11	12	

Note: The expression is high when it is over the mean value, the expression is low when it is lower than the mean value. Statistics were analyzed by Chi square test. miR-99b, microRNA-99b; miR-125a, microRNA-125a, significant difference ($P < 0.05$).

decreased in PCa cells after overexpression of miR-99b/let-7e/miR-125a cluster as well as miR-99b, let-7e, and miR-125a, respectively (**Figure 3D**, **3E**). In addition, the expression of NR6A1 was negatively correlated with that of let-7e, miR-99b, and miR-125a in patients with PCa (**Figure 3F**). These results confirm that NR6A1 is a direct target gene of miR-99b/let-7e/miR-125a, and miR-99b/let-7e/miR-125a could negatively regulate the expression of NR6A1.

Overexpression of NR6A1 promotes malignant properties of PCa cells

The functionality of NR6A1 was investigated in PCa cells through siRNA and overexpression of NR6A1. The RT-qPCR and Western blot analyses revealed a significant reduction in NR6A1 mRNA and protein expression levels when si-NR6A1-1 and si-NR6A1-2 were utilized, indicating a notable silencing effect. Conversely, overexpression of NR6A1 led to a significant increase in NR6A1 mRNA and protein expression levels (**Figure 4A**, **4B**). Transwell assays were conducted to assess the invasive and migratory abilities of the cells. The results demonstrated that overexpression of NR6A1 promoted PCa cell invasion and migration while silencing NR6A1 inhibited cell migration and invasion (**Figure 4C**). Subsequently, si1-NR6A1, which exhibited the most effective knockdown, was selected for further experiments. The findings revealed that overexpression of NR6A1 enhanced the protein expression of MMP-2, MMP-9, and VEGF, whereas silencing NR6A1 suppressed their expression (**Figure 4D**). Similarly, the EDU experiment results indicated that overexpression of NR6A1 increased the proliferative capacity of PCar cells, whereas silencing NR6A1 inhibited cell proliferation (**Figure 4E**).

NR6A1 is involved in miR-99b/let-7e/miR-125a induced PCa cell migration invasion and proliferation

To further illustrate the functional relationship between NR6A1 and miR-99b/let-7e/miR-125a, we used functional backfill experiments to illustrate that re-expression of NR6A1 in miR-99b/let-7e/miR-125a overexpressing cells affected miR-99b/let-7e/miR-125a effects on invasion and migration. Overexpression of miR-99b/let-7e/miR-125a suppressed the protein expression of NR6A1 (**Figure 5A**), restrained

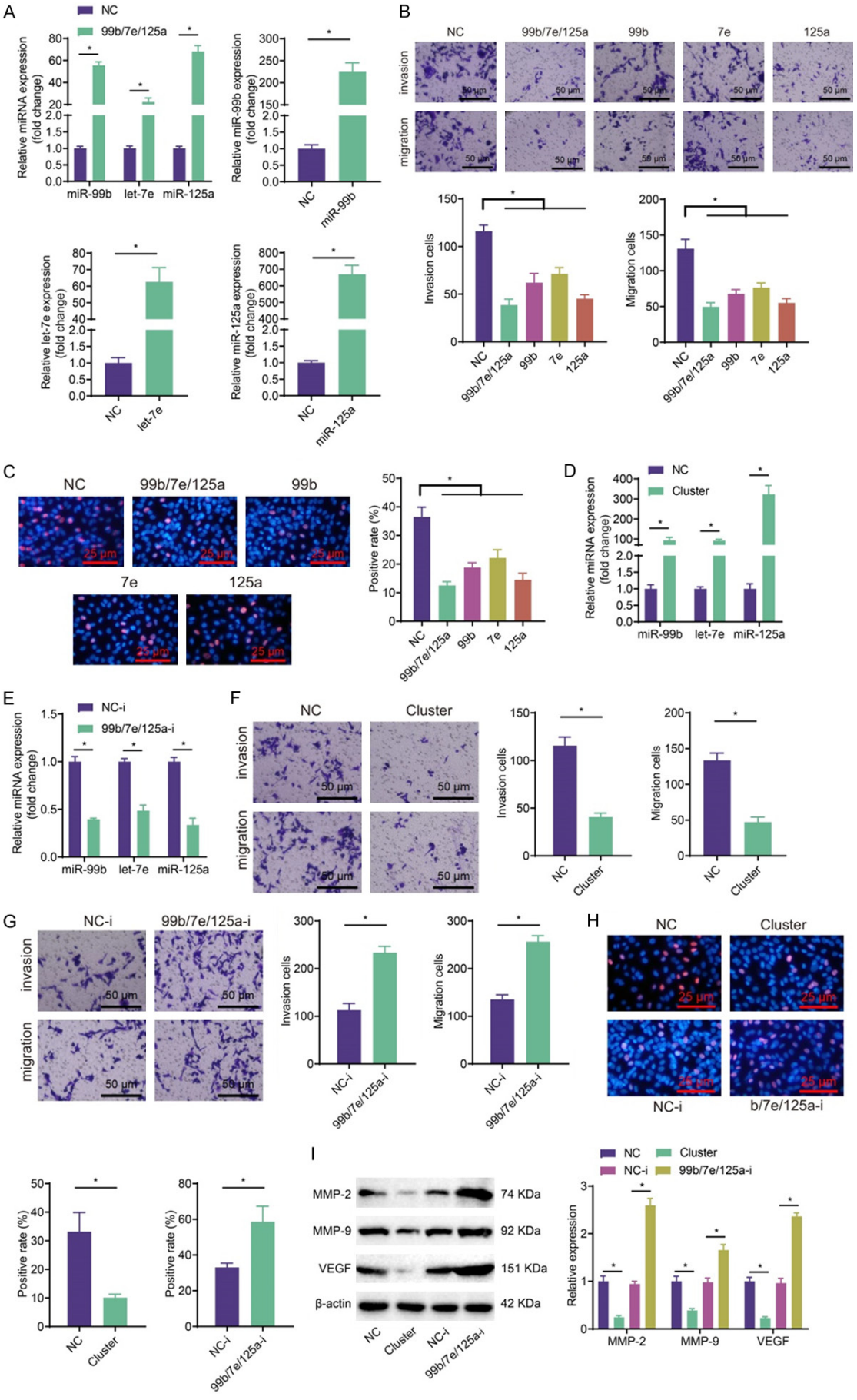
A
NC
99b/7e/125a
Relative miRNA expression (fold change)
miR-99b
let-7e
miR-125a
Relative miR-99b expression (fold change)
Relative let-7e expression (fold change)
Relative miR-125a expression (fold change)
B
NC
99b/7e/125a
99b
7e
125a
invasion
migration
50 μm
Invasion cells
Migration cells
C
25 μm
Positive rate (%)
D
Cluster
E
NC-i
99b/7e/125a-i
F
G
H
I
MMP-2
MMP-9
VEGF
β-actin
74 KDa
92 KDa
151 KDa
42 KDa
Relative expression

Figure 2. Overexpressed miR-99b/let-7e/miR-125a cluster inhibits the invasion, metastasis and proliferation of PCa cells. A. qRT-PCR is used to detect the overexpression efficiency of miR-99b/let-7e/miR-125a cluster, miR-99b, let-7e, miR-125a, and mimics. B. Transwell assay is used to investigate the invasion and migration ability of PCa cells after transfection with miR-99b/let-7e/miR-125a, miR-99b, let-7e, and miR-125a mimic. C. EdU assay is used to examine the proliferation ability of PCa cells after transfection with miR-99b/let-7e/miR-125a, miR-99b, let-7e, and miR-125a mimic. D. qRT-PCR is used to verify the overexpression efficiency of lentivirus-overexpressed miR-99b/let-7e/miR-125a. E. qRT-PCR is used to verify the knockdown efficiency of miR-99b/let-7e/miR-125a inhibitor. F. Transwell assay is used to evaluate the invasion and migration ability of PCa cells with miR-99b/let-7e/miR-125a cluster and corresponding NC. G. Transwell assay is used to evaluate the invasion and migration ability of PCa cells after addition of a combination inhibitor of miR-99b/let-7e/miR-125a and corresponding NC. H. EDU assay is used to evaluate the proliferation ability of PCa cells with miR-99b/let-7e/miR-125a cluster, miR-99b/let-7e/miR-125a-i, and corresponding NC. I. Western blot is used to detect the protein expression of metastasis-related genes in each group of PCa cells. *$P < 0.05$. A, B and F. Data are ana lyzed using one-way ANOVA. F-H. Data are analyzed using the t-test. The experiment is repeated three times.

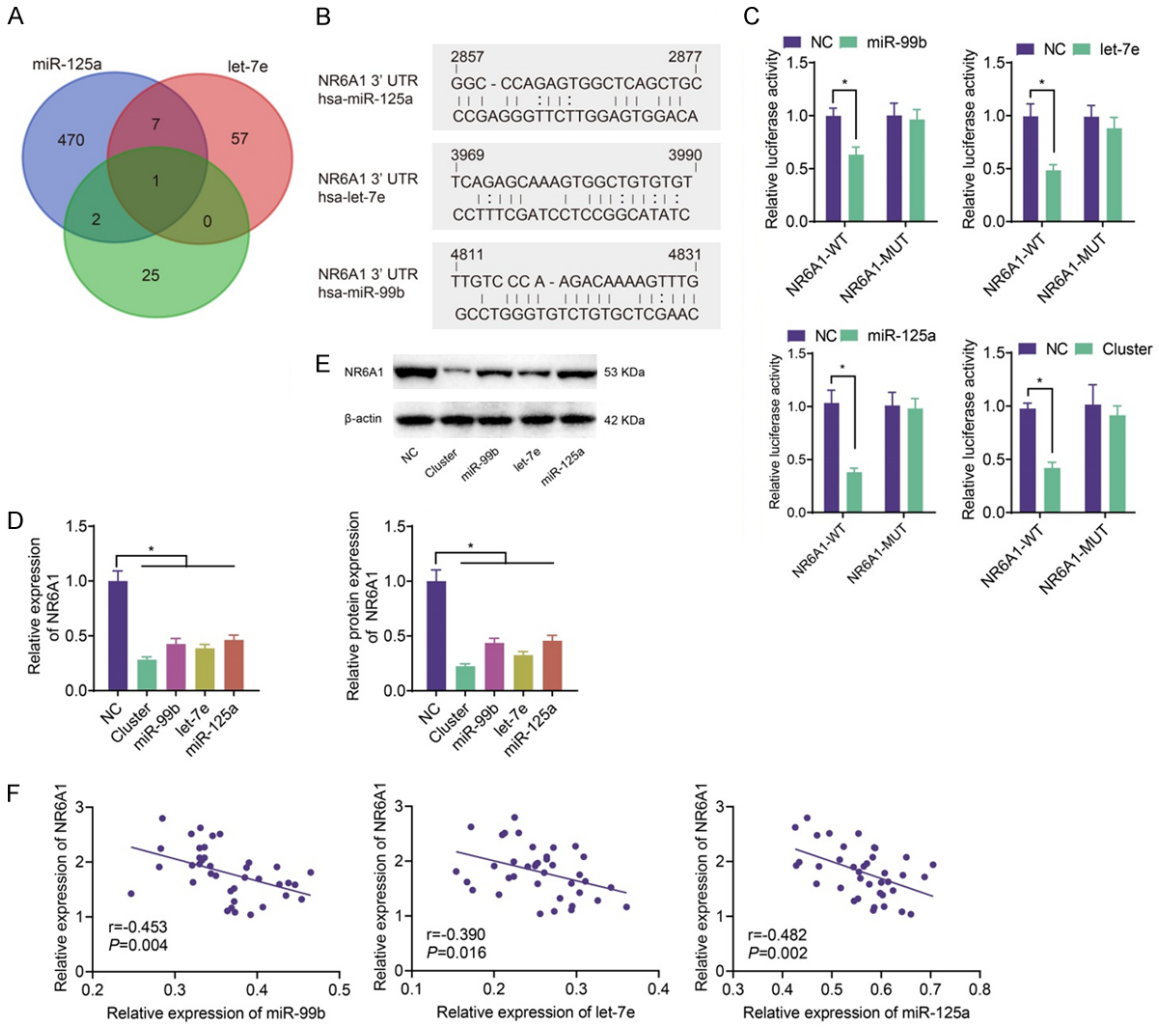

Figure 3. NR6A1 was confirmed as a direct target gene of miR-99b/let-7e/miR-125a cluster. (A) Venn diagram of the target genes of miR-125a, let-7e, and miR-99b. (B) The RNA22 prediction website predicts the binding sites existing in the 3'UTR of NR6A1 with miR-99b, let-7e, and miR-125a. (C) Dual-luciferase reporter assay is used to detect the target binding of miR-99b, let-7e, miR-125a, and miR-99b/let-7e/miR-125a cluster with NR6A1. *, $P < 0.05$ (Student's t-test). (D) RT-qPCR is used to detect the expression level of NR6A1 mRNA after overexpressing miR-99b, let-7e, and miR-125a. * *vs* NC group, $P < 0.05$. (E) Western blot is used to detect the expression of NR6A1 protein after overexpressing miR-99b, let-7e, and miR-125a. * vs NC group, $P < 0.05$. (F) The correlation between miR-99b/let-7e/miR-125a and ARID3A was examined in 78 cases of ESCC tissue samples. Data for (D and E) are analyzed using one-way ANOVA, data for (C) are analyzed using t-test, and data for (F) are analyzed using Spearman's correlation test. The experiment is repeated three times.

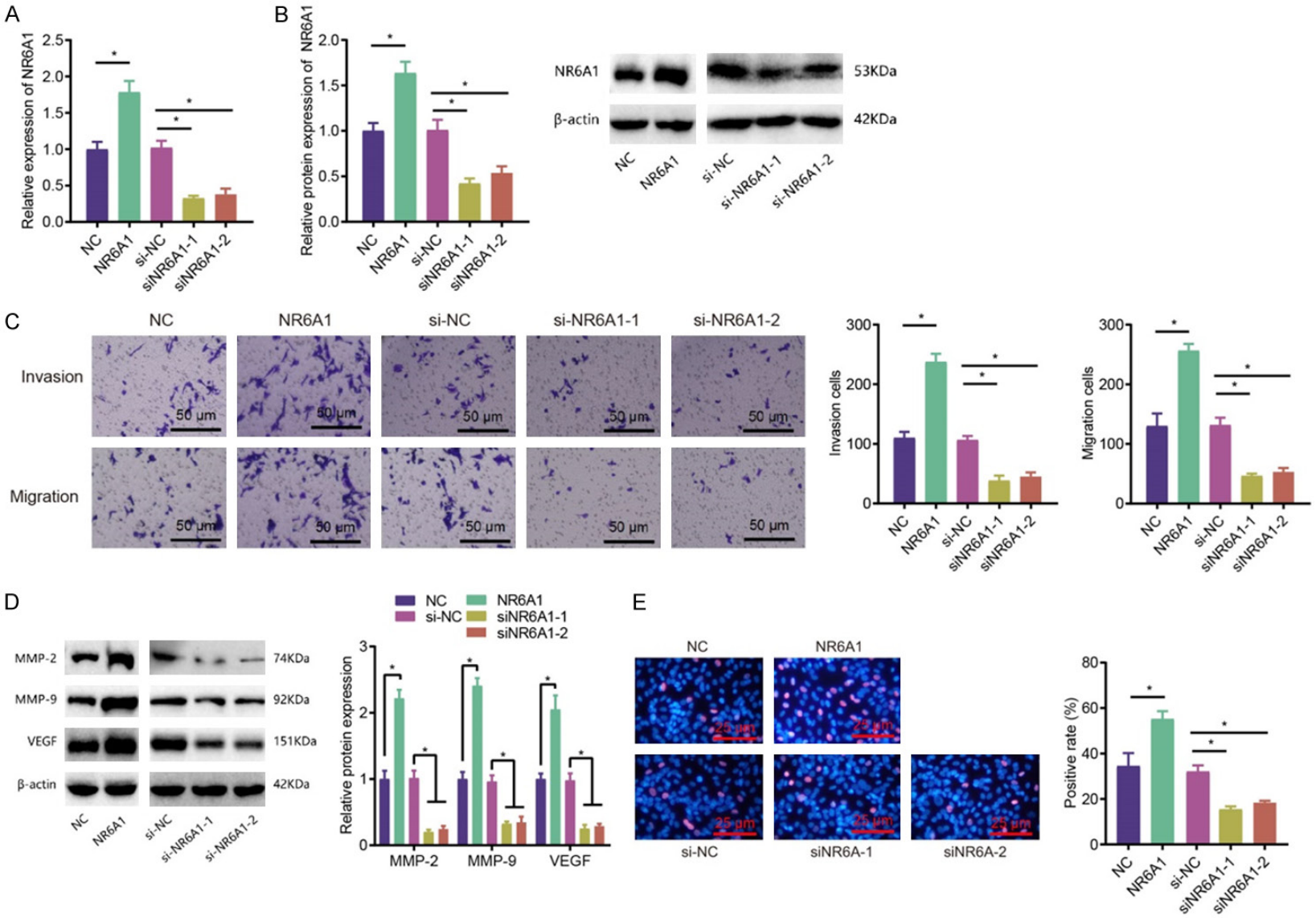

Figure 4. Overexpression of NR6A1 promotes the invasion, migration and proliferation of PCa cells. A. mRNA expression of NR6A1 in cells with overexpressed or silenced NR6A1 was detected by RT-qPCR. B. The protein expression of NR6A1 in cells with overexpressed or silenced NR6A1 was detected by Western blot analysis. C. The invasion and migration of PCa cells with overexpressed or silenced NR6A1 was determined by Transwell assay. D. The protein expression of metastasis-related genes in cells with overexpressed or silenced NR6A1 was determined by Western blot analysis. E. The proliferation of PCa cells with overexpressed or silenced NR6A1 was determined by EdU incorporation assay. * To compare the two groups depicted in the graph, a significance level of $P < 0.05$ was obtained. The data in the figure were analyzed using one-way analysis of variance (ANOVA), with three repetitions of the experiment.

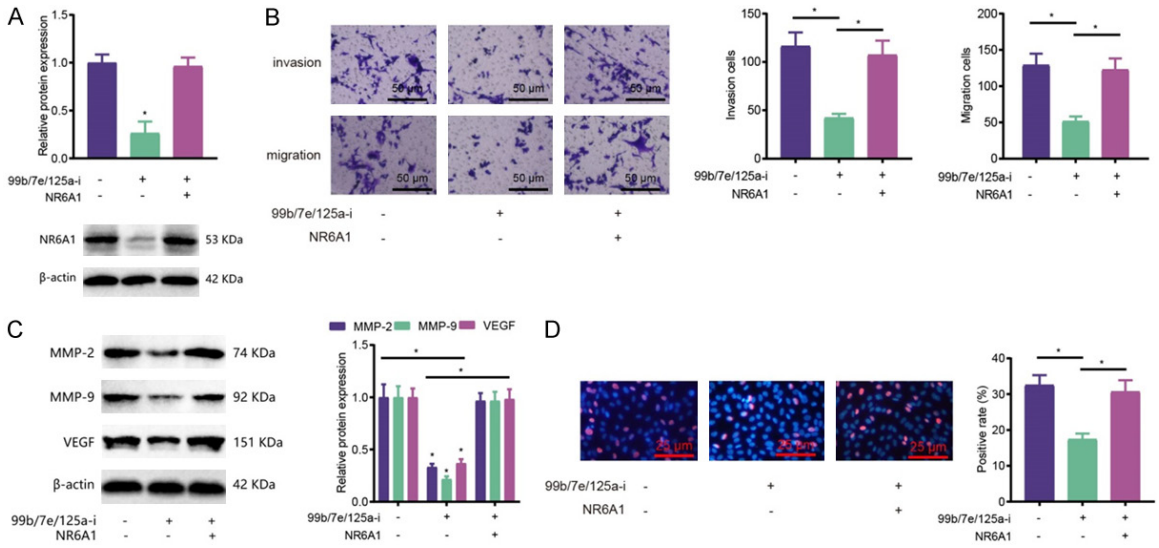

Figure 5. miR-99b/let-7e/miR-125a regulates the migration, invasion and proliferation of PCa cells by targeting NR6A1. A. Protein expression of NR6A1 in PCa cells was detected by Western blot analysis after transfection. B. The invasion and migration of PCa cells were determined by Transwell assay after transfection. C. The protein expression of MMP-2, MMP-9 and VEGF in PCa cells was detected by Western blot analysis after transfection. D. The proliferation of PCa cells was determined by EdU after transfection. * To compare the two groups depicted in the graph, a significance level of $P < 0.05$ was obtained. The data in the figure were analyzed using one-way analysis of variance (ANOVA), with three repetitions of the experiment.

the invasion, migration, and proliferation of PCa cells (**Figure 5B**), and refrained the protein expression of metastasis-related genes MMP-2, MMP-9, and VEGF (**Figure 5C**, **5D**). However, the ability of PCa cells to invade, migrate, and proliferate was restored when supplemented with overexpressed NR6A1. Therefore, NR6A1 could be an essential gene in the miR-99b/let-7e/miR-125a cluster to regulate the invasive migration and proliferative activities of PCa cells.

Effect of miR-99b/let-7e/miR-125a cluster on metastasis of PCa cells in vivo

To further determine whether the miR-99b/let-7e/miR-125a cluster can affect the activity of PCa cells, cells overexpressing this cluster were injected into nude mice to observe tumor formation and metastasis in vivo. The results of the tumorigenesis assay in nude mice showed that the overexpression of miR-99b/let-7e/miR-125a clusters resulted in smaller tumors and lighter tumor weight compared with the corresponding NC group (**Figure 6A** and **6B**). We further found that fewer liver metastatic nodules were found in the miR-99b/let-7e/miR-125a cluster than in the control group by labeling fluorescent overexpression of miR-99b/let-7e/miR-125a cluster PCa liver metastasis model (**Figure 6C** and **6D**). HE staining further confirmed the presence of liver metastasis (**Figure 6E**). Fluorescence microscopy of liver tissue revealed less green fluorescence in the liver in the overexpression miR-99b/let-7e/miR-125a cluster group compared to the NC group (**Figure 6F**). Compared with the NC mouse group, NR6A1 mRNA levels were reduced during overexpression of miR-99b/let-7e/miR-125a (**Figure 6G** and **6H**). Taken together, overexpression of miR-99b/let-7e/miR-125a cluster can inhibit the tumorigenic and the metastatic ability of PCa cells.

Discussion

PCa is a highly aggressive malignancy, often accompanied by late diagnosis and poor prognosis [20]. Many recent studies have shown that microRNAs are an important molecular mechanism regulating cancer invasion and metastasis [21]. In this study, we discovered that overexpressing the miR-99b/let-7e/miR-125a cluster significantly inhibited the invasive migration and proliferative abilities of PCa cells and decreased the expression levels of metastasis-related proteins while silencing miR-99b/let-7e/miR-125a promoted invasive migration and proliferation of PCa cells. These results powerfully demonstrate that the miR-99b/let-

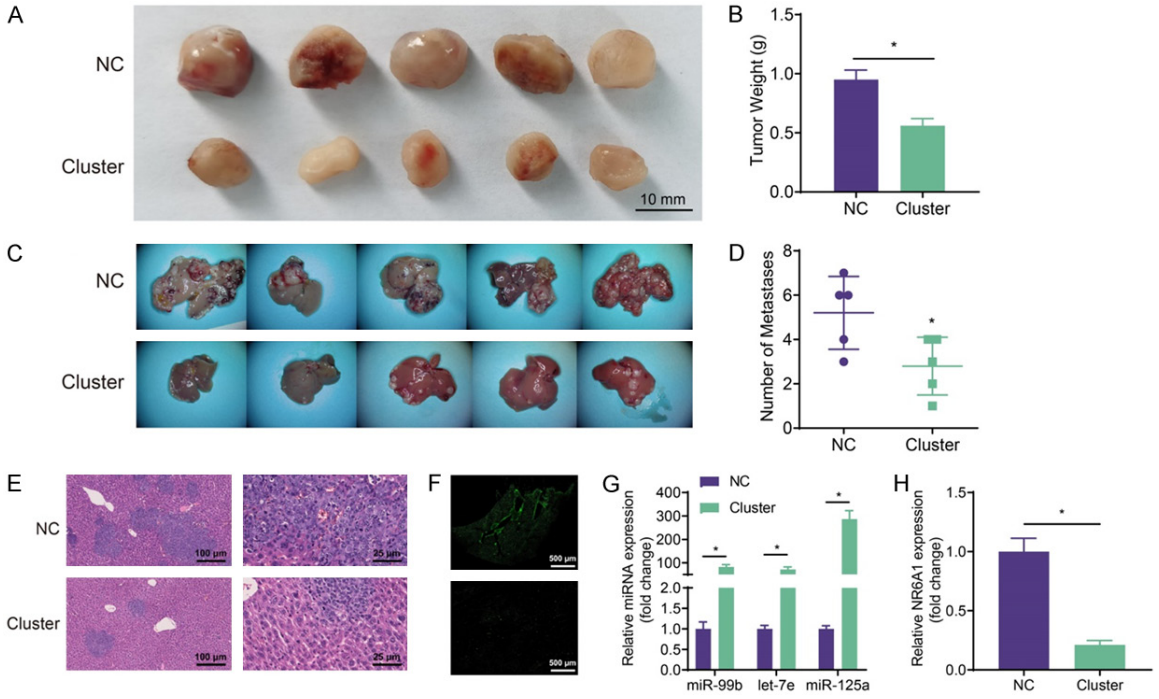

Figure 6. Overexpressed miR-99b/let-7e/miR-125a cluster inhibits the tumorigenicity and metastasis of PCa cells. A. The tumor size of nude mice with or without the miR-99b/let-7e/miR-125a cluster injected. B. Comparison of tumor weight between mice with miR-99b/let-7e/miR-125a cluster injected and the corresponding control. C. Representative photos of liver metastases using the mouse model of PCa. D. Statistical analysis of liver metastasis. E. HE staining of the paraffin-embedded sections of liver metastatic nodules. Scar bars, 500 μm (left) and 200 μm (right). F. Fluorescence images of PCa cells labeled by DAPI in frozen mouse liver sections. Scar bar, 500 μm. G. Quantitative real-time polymerase chain reaction (qRT-PCR) to assess the expression levels of miR-99b, let-7e, and miR-125a in the tissues. H. qRT-PCR to measure the expression levels of NR6A1 in the tissues. Data are presented as mean ± standard deviation (SD). *$P < 0.05$ was determined by conducting a t-test analysis on the data shown in the graph, with three repetitions of the experiment. N = 5.

7e/miR-125a cluster is vital in regulating PCa invasion and metastasis and that this role is mediated through its common target gene NR6A1. Therefore, this cluster and NR6A1 may be potential targets for regulating PCa invasion and metastasis through miRNAs, providing new strategies and directions for treating PCa.

Our study also indicated that low expression levels of miR-125a, let-7e, and miR-99b in PCa patients were negatively correlated with the development of pancreatic tumors as some miR or oncoming, miR-125a, let-7e, and miR-99b are important potential tumor suppressors [22]. The overexpression of miR-125a or miR-125b exerted minor effects on the growth and migration of untransformed human breast epithelial cells, suggesting the potential of mir as a therapeutic strategy to block oncogene expression and function [23]. Another study noted that miR-125a promotes chemotherapy resistance of PCa cells to gemcitabine by targeting A20, suggesting that miR-125a may serve as a novel therapeutic target or molecular indicator for prostate cancer treatment and may improve the diagnosis of prostate cancer [24]. It was shown that miR-125a controls the size of the stem cell population by regulating hematopoietic stem/progenitor cell (HSPC) apoptosis [25]. For miR-let-7e, previous studies have shown that JARID1B demethylase promotes tumor cell proliferation by epigenetically inhibiting the tumor suppressor miR-let-7e [26]. Another study suggested that let-7e may serve as a promising therapeutic target for improving the sensitivity of cisplatin-resistant human epithelial ovarian cancer to cisplatin [27]. Similarly, the miR-99 family, including miR-99a, -99b, and -100, inhibits prostate-specific antigen expression and prostate cancer cell proliferation [28]. Another study demonstrated that miR-99b, by targeting mTOR induction, contributes to the irradiation resistance of PCa [29]. Previous studies confirmed that the miR-125a/

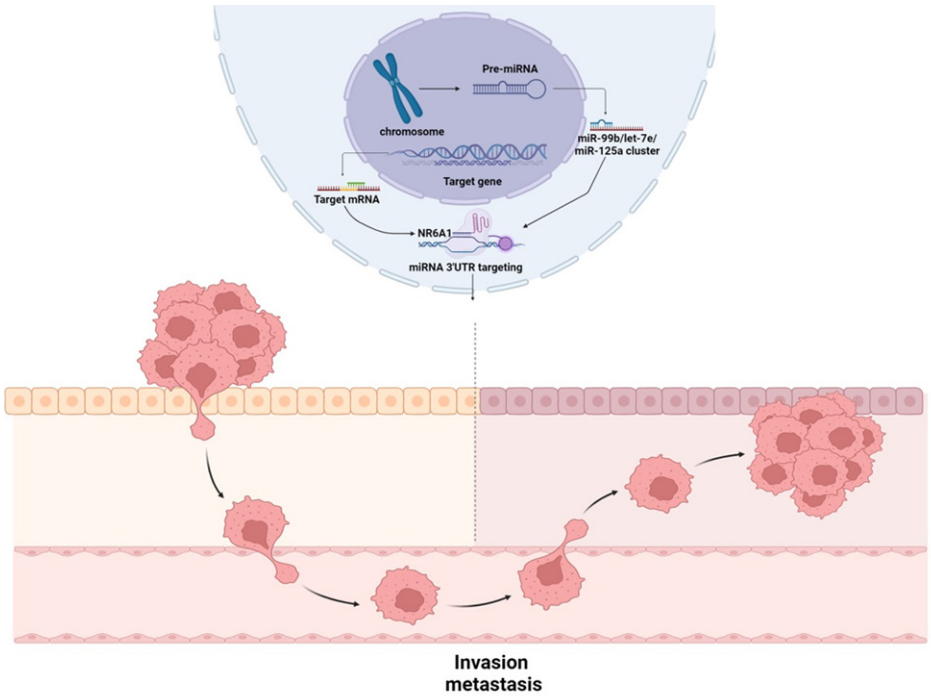

Figure 7. NR6A1 is the target gene of the miR-99b/let-7e/miR-125a and is negatively regulated by them, confirmed by the bioinformatics prediction and dual luciferase reporter gene assay. The miR-99b/let-7e/miR-125a cluster, which is closely adjacent to each other on a chromosome, is transported by the precursor miRNA from the nucleus to the nucleus and into the cytoplasm to inhibit NR6A1 expression, thus affecting the invasion and metastasis of PCa cells.

let-7e/-miR-99b cluster might be involved in the pathogenesis of cystic fibrosis [30].

We also demonstrated that the expression of MMP-2, MMP-9, and VEGF was significantly reduced in miR-99b/let-7e/miR-125a overexpressed cells, suggesting that their overexpression could inhibit the invasion and metastasis of PCa cells in vitro. Previous studies found that the expression of MMP-2, MMP-9, and VEGF was positively correlated with metastasis, invasion, growth, and angiogenesis of gastric cancer cells, suggesting their potential role in predicting the pathobiological behavior of gastric cancer [31]. Previous studies confirmed that miRNA-21 plays an active role in angiogenesis by promoting cell survival, migration, and tube formation [32]. It can also inhibit cell death by partially targeting TIMP3 and regulating MMP92 and MMP [33]. Another study showed that miR let-7e acts as a differentiation inducer and stromal MMP9 inhibitor in adipose-derived stem cells [34]. In addition, previous studies have shown that post-transcriptional processing of mRNA transcripts plays a crucial role in establishing cellular gene expression profiles [35]. In our study, we searched for mir targeting ORL1 [36]. The results of the prediction website (http://www.microrna.org) and the dual luciferase reporter gene assay confirmed NR6A1 as a direct target gene of the miR-99b/let-7e/miR-125a cluster. Previous literature has demonstrated that cellular levels of NR6A1 correlate with disease progression in prostate cancer, suggesting that this essential orphan nuclear receptor may be a potential therapeutic target and a novel biomarker of prostate cancer aggressiveness [37]. Similar results were obtained in our study. In addition, NR6A1, an embryonic transcriptional negative regulator of gene expression in adult fibroblasts, has been reported to be repressed by let-7 [38].

In this study, bioinformatics tools were used to screen the miR-99b/let-7e/miR-125a cluster for its association with PCa, and the expected

target gene of these three miRNAs was NR6A1. The experimental results showed that the miR-99b/let-7e/miR-125a cluster could reduce the expression of NR6A1, thus inhibiting the invasion and metastasis of PCa cells (**Figure 7**). This finding increases the understanding of the mechanism of PCa development and progression and is expected to provide new possibilities and directions for PCa treatment. While this study established that the miR-99b/let-7e/miR-125a cluster could inhibit PCa invasion and metastasis via NR6A1, further investigation and validation of other potential target molecules are required. Additionally, extensive clinical sample analysis is necessary to support the application of these findings in clinical settings.

Acknowledgements

This work is supported by the General Project of Zhejiang Health Science and Technology Plan (2021KY1150 and 2023KY1234), and the Project of Shaoxing Health and Technology Plan (2022SY014).

Informed consent was obtained from each participant.

Disclosure of conflict of interest

None.

Address correspondence to: Zhiqiang Lin, Department of Vascular Hernia Surgery, Shaoxing People's Hospital, No. 568, Zhongxing North Road, Shaoxing 312000, Zhejiang, P. R. China. Tel: +86-13735375063; E-mail: 13735375063@163.com

References

[1] Tian Y, Tang B, Wang C, Wang Y, Mao J, Yao Y, Gao Z, Liang R, Ye M, Cai S and Wang L. Operative ubiquitin-specific protease 22 deubiquitination confers a more invasive phenotype to cholangiocarcinoma. Cell Death Dis 2021; 12: 678.

[2] Ramchandani M, Lakhtakia S, Costamagna G, Tringali A, Puspoek A, Tribl B, Dolak W, Deviere J, Arvanitakis M, van der Merwe S, Laleman W, Ponchon T, Lepilliez V, Gabbrielli A, Bernardoni L, Bruno MJ, Poley JW, Arnelo U, Lau J, Roy A, Bourke M, Kaffes A, Neuhaus H, Peetermans J, Rousseau M and Reddy DN. Fully covered self-expanding metal stent vs multiple plastic stents to treat benign biliary strictures secondary to chronic pancreatitis: a multicenter randomized trial. Gastroenterology 2021; 161: 185-195.

[3] Shah R and John S. Cholestatic Jaundice. In: StatPearls. Treasure Island (FL): StatPearls Publishing; 2023.

[4] Zerem E, Imsirovic B, Kunosic S, Zerem D and Zerem O. Percutaneous biliary drainage for obstructive jaundice in patients with inoperable, malignant biliary obstruction. Clin Exp Hepatol 2022; 8: 70-77.

[5] Ramanand SG, Chen Y, Yuan J, Daescu K, Lambros MB, Houlahan KE, Carreira S, Yuan W, Baek G, Sharp A, Paschalis A, Kanchwala M, Gao Y, Aslam A, Safdar N, Zhan X, Raj GV, Xing C, Boutros PC, de Bono J, Zhang MQ and Mani RS. The landscape of RNA polymerase II-associated chromatin interactions in prostate cancer. J Clin Invest 2020; 130: 3987-4005.

[6] Masetti M, Carriero R, Portale F, Marelli G, Morina N, Pandini M, Iovino M, Partini B, Erreni M, Ponzetta A, Magrini E, Colombo P, Elefante G, Colombo FS, den Haan JMM, Peano C, Cibella J, Termanini A, Kunderfranco P, Brummelman J, Chung MWH, Lazzeri M, Hurle R, Casale P, Lugli E, DePinho RA, Mukhopadhyay S, Gordon S and Di Mitri D. Lipid-loaded tumor-associated macrophages sustain tumor growth and invasiveness in prostate cancer. J Exp Med 2022; 219: e20210564.

[7] Culig Z. miRNA as regulators of prostate carcinogenesis and endocrine and chemoresistance. Curr Cancer Drug Targets 2021; 21: 283-288.

[8] Zhao J, Ma X and Xu H. miR-29b-3p inhibits 22Rv1 prostate cancer cell proliferation through the YWHAE/BCL-2 regulatory axis. Oncol Lett 2022; 24: 289.

[9] Singhi AD and Wood LD. Early detection of pancreatic cancer using DNA-based molecular approaches. Nat Rev Gastroenterol Hepatol 2021; 18: 457-468.

[10] Shin J, Seo N, Baek SE, Son NH, Lim JS, Kim NK, Koom WS and Kim S. MRI radiomics model predicts pathologic complete response of rectal cancer following chemoradiotherapy. Radiology 2022; 303: 351-358.

[11] Dai SM, Li FJ, Long HZ, Zhou ZW, Luo HY, Xu SG and Gao LC. Relationship between miRNA and ferroptosis in tumors. Front Pharmacol 2022; 13: 977062.

[12] Eniafe J and Jiang S. MicroRNA-99 family in cancer and immunity. Wiley Interdiscip Rev RNA 2021; 12: e1635.

[13] Sartor O, de Bono J, Chi KN, Fizazi K, Herrmann K, Rahbar K, Tagawa ST, Nordquist LT, Vaishampayan N, El-Haddad G, Park CH, Beer TM, Armour A, Perez-Contreras WJ, DeSilvio M, Kpamegan E, Gericke G, Messmann RA, Morris MJ and Krause BJ; VISION Investigators.

Lutetium-177-PSMA-617 for metastatic castration-resistant prostate cancer. N Engl J Med 2021; 385: 1091-1103.
[14] Hsu AC, Dua K, Starkey MR, Haw TJ, Nair PM, Nichol K, Zammit N, Grey ST, Baines KJ, Foster PS, Hansbro PM and Wark PA. MicroRNA-125a and -b inhibit A20 and MAVS to promote inflammation and impair antiviral response in COPD. JCI Insight 2017; 2: e90443.
[15] Dika E, Broseghini E, Porcellini E, Lambertini M, Riefolo M, Durante G, Loher P, Roncarati R, Bassi C, Misciali C, Negrini M, Rigoutsos I, Londin E, Patrizi A and Ferracin M. Unraveling the role of microRNA/isomiR network in multiple primary melanoma pathogenesis. Cell Death Dis 2021; 12: 473.
[16] Sun L, Zhu M, Feng W, Lin Y, Yin J, Jin J and Wang Y. Exosomal miRNA Let-7 from menstrual blood-derived endometrial stem cells alleviates pulmonary fibrosis through regulating mitochondrial DNA damage. Oxid Med Cell Longev 2019; 2019: 4506303.
[17] Ma J, Zhan Y, Xu Z, Li Y, Luo A, Ding F, Cao X, Chen H and Liu Z. ZEB1 induced miR-99b/let-7e/miR-125a cluster promotes invasion and metastasis in esophageal squamous cell carcinoma. Cancer Lett 2017; 398: 37-45.
[18] Zhou W, Jiang R, Wang Y, Li Y, Sun Z and Zhao H. hsa_circ_001653 up-regulates NR6A1 expression and elicits gastric cancer progression by binding to microRNA-377. Exp Physiol 2020; 105: 2141-2153.
[19] Smyth GK. Linear models and empirical Bayes methods for assessing differential expression in microarray experiments. Stat Appl Genet Mol Biol 2004; 3: Article3.
[20] Wang X, Luo G, Zhang K, Cao J, Huang C, Jiang T, Liu B, Su L and Qiu Z. Hypoxic tumor-derived exosomal miR-301a mediates M2 macrophage polarization via PTEN/PI3Kgamma to promote pancreatic cancer metastasis. Cancer Res 2018; 78: 4586-4598.
[21] Cai S, Pataillot-Meakin T, Shibakawa A, Ren R, Bevan CL, Ladame S, Ivanov AP and Edel JB. Single-molecule amplification-free multiplexed detection of circulating microRNA cancer biomarkers from serum. Nat Commun 2021; 12: 3515.
[22] Wang QW, Sun YN, Tan LJ, Zhao JN, Zhou XJ, Yu TJ and Liu JT. MiR-125 family improves the radiosensitivity of head and neck squamous cell carcinoma. Mol Biol Rep 2023; 50: 5307-5317.
[23] Gerasymchuk M, Cherkasova V, Kovalchuk O and Kovalchuk I. The role of microRNAs in organismal and skin aging. Int J Mol Sci 2020; 21: 5281.
[24] Liu JZ, Yin FY, Yan CY, Wang H and Luo XH. Regulation of docetaxel sensitivity in prostate cancer cells by hsa-miR-125a-3p via modulation of metastasis-associated protein 1 signaling. Urology 2017; 105: 208.e11-208.e17.
[25] Bujko K, Kucia M, Ratajczak J and Ratajczak MZ. Hematopoietic stem and progenitor cells (HSPCs). Adv Exp Med Biol 2019; 1201: 49-77.
[26] Wu S, Ren K, Zhao J, Li J, Jia B, Wu X, Dou Y, Fei X, Huan Y, He X, Wang T, Lv W, Wang L, Wang Y, Zhao J, Fei Z and Li S. LncRNA GAS5 represses stemness and malignancy of gliomas via elevating the SPACA6-miR-125a/let-7e axis. Front Oncol 2022; 12: 803652.
[27] Moore KN, Oza AM, Colombo N, Oaknin A, Scambia G, Lorusso D, Konecny GE, Banerjee S, Murphy CG, Tanyi JL, Hirte H, Konner JA, Lim PC, Prasad-Hayes M, Monk BJ, Pautier P, Wang J, Berkenblit A, Vergote I and Birrer MJ. Phase III, randomized trial of mirvetuximab soravtansine versus chemotherapy in patients with platinum-resistant ovarian cancer: primary analysis of FORWARD I. Ann Oncol 2021; 32: 757-765.
[28] Van Poppel H, Roobol MJ, Chapple CR, Catto JWF, N'Dow J, Sonksen J, Stenzl A and Wirth M. Prostate-specific antigen testing as part of a risk-adapted early detection strategy for prostate cancer: European Association of Urology Position and Recommendations for 2021. Eur Urol 2021; 80: 703-711.
[29] Niture S, Tricoli L, Qi Q, Gadi S, Hayes K and Kumar D. MicroRNA-99b-5p targets mTOR/AR axis, induces autophagy and inhibits prostate cancer cell proliferation. Tumour Biol 2022; 44: 107-127.
[30] Recchiuti A, Patruno S, Mattoscio D, Isopi E, Pomilio A, Lamolinara A, Iezzi M, Pecce R and Romano M. Resolvin D1 and D2 reduce SARS-CoV-2-induced inflammatory responses in cystic fibrosis macrophages. FASEB J 2021; 35: e21441.
[31] Shi A, Wang T, Jia M, Dong L and Shi H. Effects of SDF-1/CXCR7 on the migration, invasion and epithelial-mesenchymal transition of gastric cancer cells. Front Genet 2021; 12: 760048.
[32] Gao J, Wang S, Zhang Z and Li J. Long noncoding RNA BRE-AS1 inhibits the proliferation, migration, and invasion of cancer cells in triple-negative breast cancer and predicts patients' survival by downregulating miR-21. BMC Cancer 2021; 21: 745.
[33] Zhang D, Lu W, Cui S, Mei H, Wu X and Zhuo Z. Establishment of an ovarian cancer omentum metastasis-related prognostic model by integrated analysis of scRNA-seq and bulk RNA-seq. J Ovarian Res 2022; 15: 123.
[34] Ginckels P and Holvoet P. Oxidative stress and inflammation in cardiovascular diseases and

cancer: role of non-coding RNAs. Yale J Biol Med 2022; 95: 129-152.
[35] Ali Syeda Z, Langden SSS, Munkhzul C, Lee M and Song SJ. Regulatory mechanism of MicroRNA expression in cancer. Int J Mol Sci 2020; 21: 1723.
[36] Gopalakrishnan L, Chatterjee O, Ravishankar N, Suresh S, Raju R, Mahadevan A and Prasad TSK. Opioid receptors signaling network. J Cell Commun Signal 2022; 16: 475-483.
[37] Zheng Y, Gao Y, Li X, Si S, Xu H, Qi F, Wang J, Cheng G, Hua L and Yang H. Long non-coding RNA NAP1L6 promotes tumor progression and predicts poor prognosis in prostate cancer by targeting Inhibin-beta A. Onco Targets Ther 2018; 11: 4965-4977.
[38] Tan P, Xue T, Wang Y, Hu Z, Su J, Yang R, Ji J, Ye M, Chen Z, Huang C and Lu X. Hippocampal NR6A1 impairs CREB-BDNF signaling and leads to the development of depression-like behaviors in mice. Neuropharmacology 2022; 209: 108990.